Journal of Natural Products
Vol. 48, No. 2, pp. 173-192, Mar-Apr 1985

NATURAL PRODUCTS AS PROBES FOR NUCLEIC ACID STRUCTURE AND SEQUENCE[1]

WILLIAM A. REMERS

Department of Pharmaceutical Sciences, College of Pharmacy, University of Arizona, Tucson, Arizona 85721

ABSTRACT.—Double helical DNA exists in a dynamic equilibrium among various forms, including partially unwound ones. The binding of molecules, including drugs and other natural products, influences this equilibrium. It produces changes in the physical properties of both the molecule and the DNA. Chemical changes such as covalent binding and DNA strand scission also occur. These changes can affect the replication and transcription of the DNA. The specific sites at which drugs bind to DNA can be determined by sequencing methods, including the Maxam-Gilbert and the "footprinting" technique of Galas and Schmitz.

DNA STRUCTURE.—A variety of different forms have been found for isolated double helical DNA. The existence of a particular form depends on the environment of the DNA, and transitions from one form into another can be brought about by changing the environment. Thus, the family of A forms of DNA exists in air at a relative humidity of 75%. It also exists in aqueous solution containing a high proportion (70-80%) of EtOH (1). In ordinary aqueous solution at low ionic strength, the familiar B family is present. The differences between the A and B forms of DNA is shown in Figure 1. Both forms have the right-handed double helix, but there is a difference in stacking of the base pairs. In B-DNA, the base pairs are at the central axis and almost perpendicular to it, whereas in A-DNA, the base pairs are removed from the central axis and tilted by 19° from it. The minor groove of A-DNA is flatter and wider than that of B-DNA, whereas the corresponding major groove is deeper, extending through the axis (2). These differences reflect different conformations in the deoxyribose units of the DNA. As shown in Figure 2, the C-3′ *endo*-conformation is present in A-DNA and the C-2′ *endo*-conformation exists in B-DNA (3).

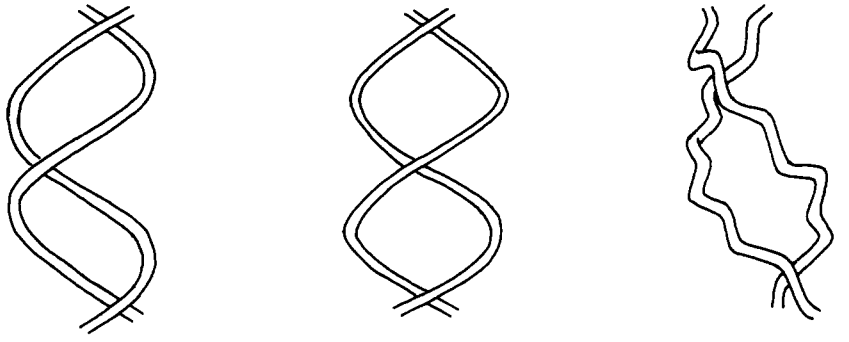

FIGURE 1. Comparisons of A, B, and Z forms of DNA.

If a solution of B-DNA is treated with increasing concentrations of salt, regions containing alternating purines and pyrimidines will be converted into Z-DNA. This Z-form also is a double helix with base pairs nearly perpendicular to the axis, but the base pairs are removed from the central axis. Conformations of the sugars alternate between

[1]Presented as a plenary lecture at the "Biotechnology in Natural Products Research" Symposium of the 25th Annual Meeting of the American Society of Pharmacognosy at the University of Texas, Austin, Texas, August 19-23, 1984.

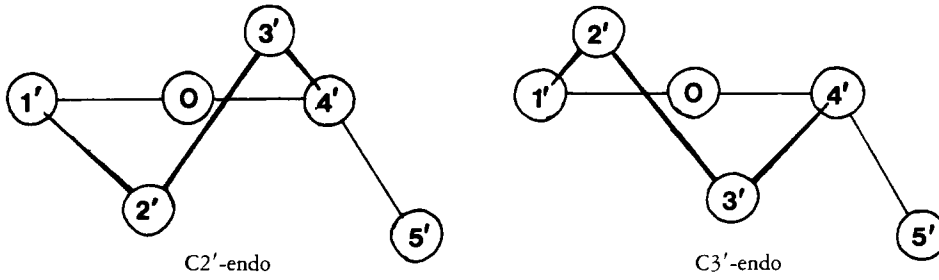

FIGURE 2. Conformations of the 2'-deoxyribose units in A and B forms of DNA. After Wang, *et al.* (3).

the C-2' *endo*-pucker with C-4', C-5' *gauche-gauche* bond and *syn*-base, such as found in B-DNA, and a novel C-3' *endo*-pucker with C-4', C-5' *gauche-trans* bond and *anti*-base. This pattern results in a zig-zag arrangement of phosphates and a left-handed double helix (Figure 1) (4). Thus, the chirality of the helix is opposite to that of B-DNA. The circular dichroism spectra of the two forms (Figure 3) clearly show this reversal of chirality. Another significant difference between the two forms is the thinner profile of Z-DNA.

The studies of DNA structure described above were made on isolated DNA. However, chemotherapy and carcinogenesis are concerned with interactions between natural and unnatural substances and chromosomal DNA. The existence of various forms of DNA in chromosomes is not well-defined. However, it is thought that a dynamic equilibrium occurs among different forms of histone-DNA complexes (5), perhaps involving unwinding of the β-helix at localized β-kinked structures (6).

ALKYLATION OF DNA.—Alkylation of DNA involves the formation of a covalent bond between a nucleophilic atom on the DNA and a carbon atom on the alkylating agent. This kind of transformation can have serious consequences for a cell, producing mutagenesis or cell death if the DNA cannot be repaired efficiently. One example of a carcinogenic agent is aflatoxin B_1. As shown in Scheme 1, this fungal product is con-

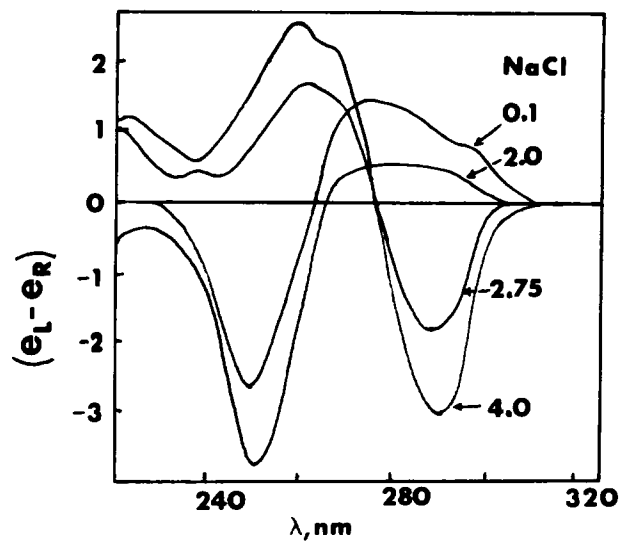

FIGURE 3. Circular dichroism spectra of B-DNA in the presence of increasing concentrations of salt. A transformation into the Z form occurs at higher concentrations. After Nordheim, *et al.* (7). Permission from American Association for the Advancement of Science.

verted in the body to its highly reactive 2,3-epoxide, which is attacked by the nucleophilic N^7 of a deoxyguanosine residue of DNA. The resulting alkylated DNA cannot be converted from the B into the Z form by increasing salt concentration (7).

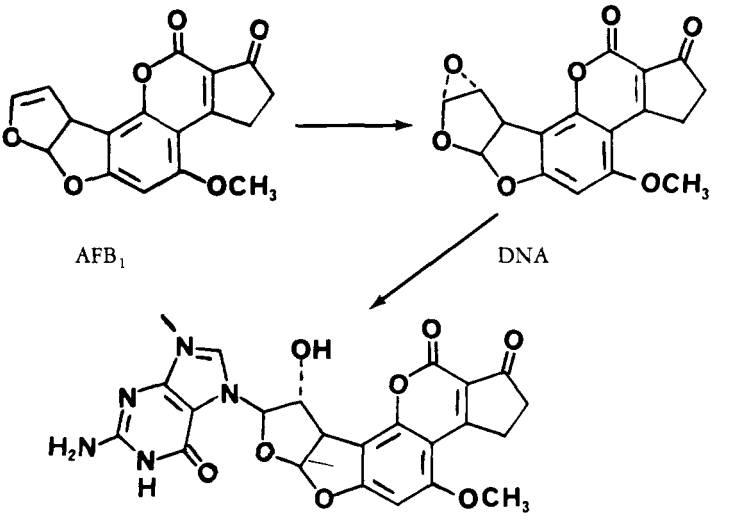

SCHEME 1. Biotransformation of aflatoxin B_1 and DNA alkylation by the resulting epoxide.

Methylation of DNA also results in mutagenesis. Among its effects on DNA, methylation of N^7 of guanine provides a means for the selective cleavage of a strand with loss of an N^7-methylguanine residue. This process is used to advantage in the Maxam-Gilbert DNA sequencing method, which will be described in detail later in this article. A recent ^{13}C-nmr study on the methylation and alkaline hydrolysis of DNA has provided a clear picture of the guanine selective cleavage (8). In this study, DNA was treated with ^{13}C-dimethyl sulfate and the ^{13}C-nmr spectrum was taken before and after alkaline hydrolysis. Figure 4 shows that the principal sites of methylation were on N^7 of deoxyguanosine, N^1 of deoxyadenosine, N^3 of deoxycytosine, and phosphate oxygen. After alkaline hydrolysis, very little N^7-methyldeoxyguanosine is present, but much N^7-methylguanine has been liberated. A significant change also has occurred in N^1-methyldeoxyadenosine; however, free N^1-methyladenine has not been formed. Instead, a rearrangement to N^6-methyl-deoxyadenosine, still bound to the DNA, has occurred. The chemical reactions involved in the methylation and further transformation of the deoxyguanosine and deoxyadenosine residues are shown in Schemes 2 and 3, respectively. It should be noted that previous schemes offered for the hydrolysis of N^7-methyldeoxyguanosine had an attack of H_2O or hydroxide ion on C^8, with opening of the imidazole ring and formation of an N^9-formyl derivative. No evidence for this process was found in the study just described (8).

Most alkylating agents that have significant antitumor activity are capable of bifunctional alkylation. The bifunctional alkylation of double helical DNA can be either interstrand or intrastrand. In the case of interstrand alkylation, the two strands of the DNA are covalently linked to each other through the alkylating agent. Such cross linked DNA can be detected readily by a test based on heat denaturation followed by cooling and treatment with S_1-endonuclease (9). Unreacted or monoalkylated DNA will undergo separation of the two strands of the helix when heated. Upon cooling, their recombination will be a slow process, and the separated strands can be cleaved into small fragments by the endonuclease. In contrast, the cross linked DNA strands will renature quickly and resist cleavage by S_1-endonuclease (Figure 5).

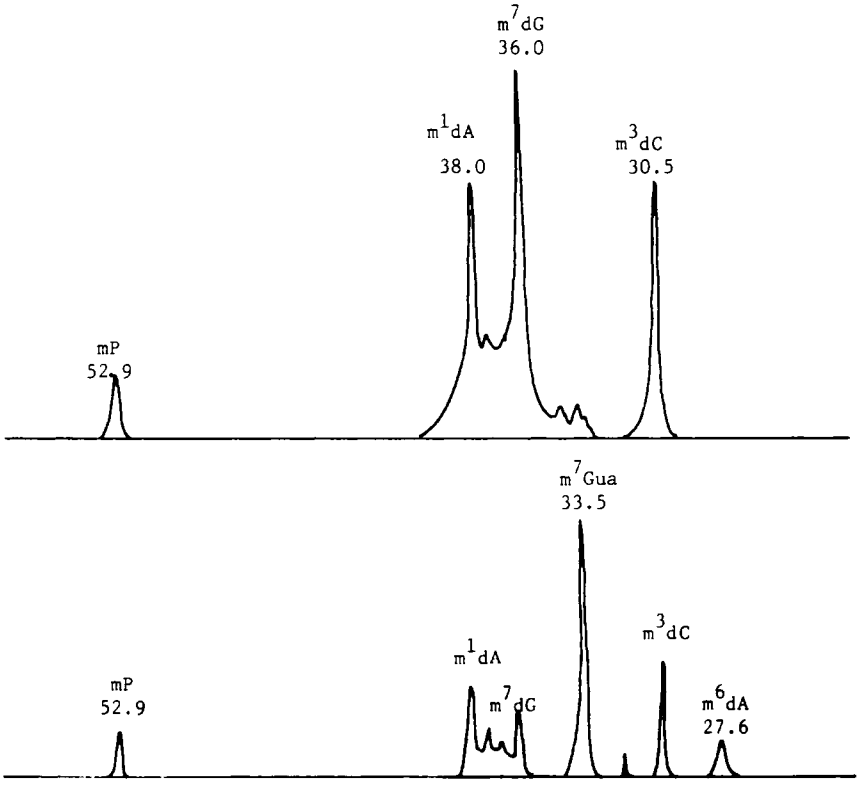

FIGURE 4. ^{13}C-nmr spectrum of methylated DNA before and after alkaline hydrolysis. After Chang, *et al.* (8). Permission from American Chemical Society.

Mitomycin C is an example of a natural product that cross links DNA. This antitumor antibiotic is not a good alkylating agent until it is activated by reduction to the corresponding semiquinone or hydroquinone (10). A variety of biological systems, for instance, the NADPH-cytochrome P-450 system, can produce this bioreductive activation (11). The initially formed reactive intermediate losses the elements of MeOH to give a mitosene, which is the alkylating species (Scheme 4). Single strand alkylation of

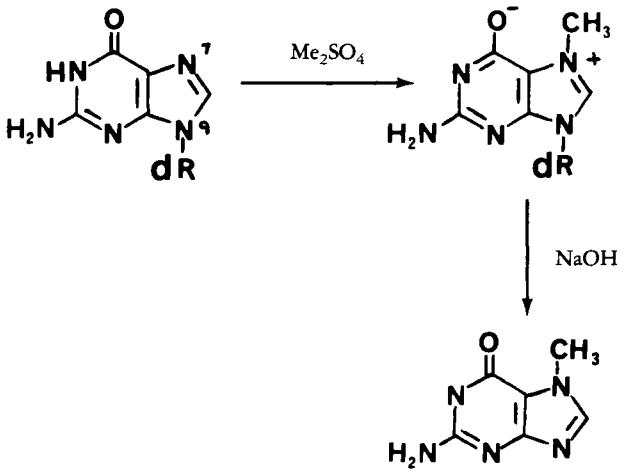

SCHEME 2. Chemical transformation of 2′-deoxyguanosine on methylation and alkaline hydrolysis.

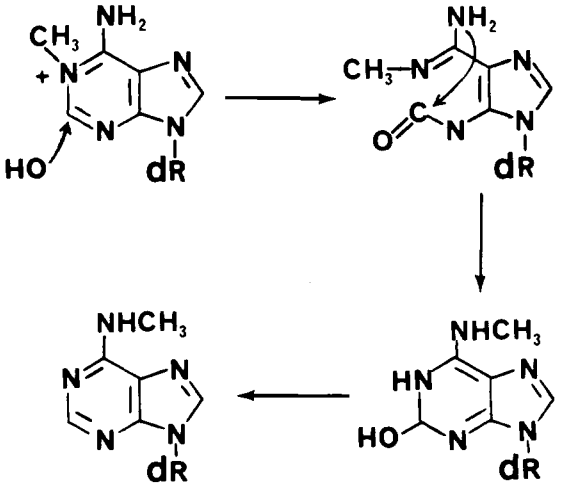

SCHEME 3. Chemical transformation of 2'-deoxyadenosine on methylation and alkaline hydrolysis.

DNA involves primarily covalent bond formation between O-6 of a guanine residue and C-1 of the mitosene (12,13). The second alkylation sites involved in cross linking have not yet been established. One reasonable postulated structure based on model building features covalent bonding to O-6 of guanine on both DNA strands with C-1 and C-10 of the mitosene (Figure 6) (14).

INTERCALATION INTO DNA.—A significant number of antitumor drugs, including important ones such as doxorubicin (Adriamycin), bind to DNA by intercalation (15,16). The intercalation process involves partial unwinding of the double helix to

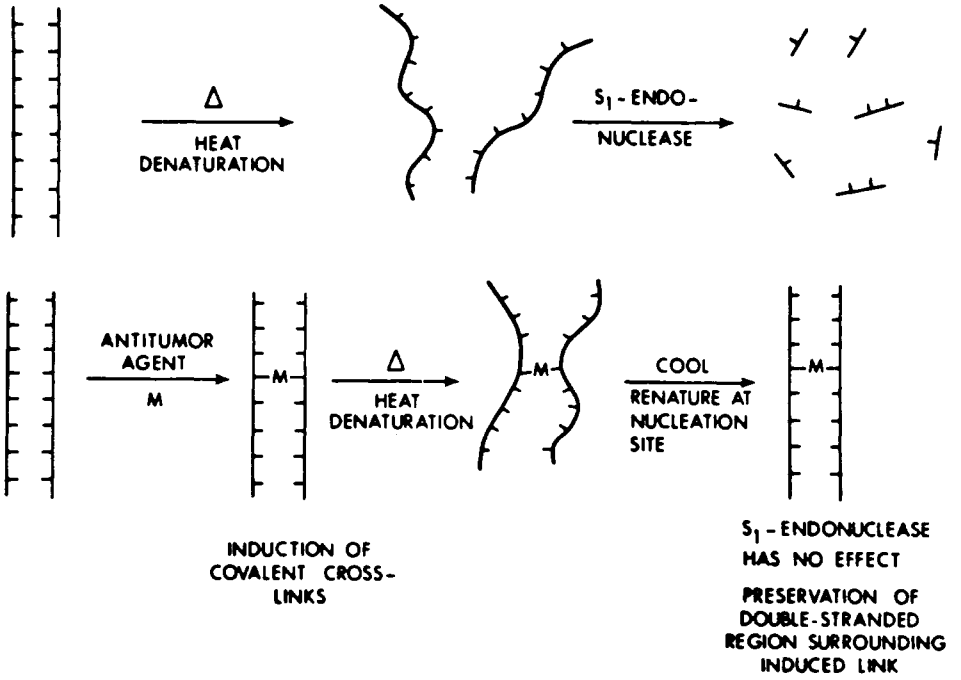

FIGURE 5. The effect of DNA crosslinking on heat denaturation and treatment with S_1 endonuclease. Reproduced from Lown (9). Permission from Academic Press.

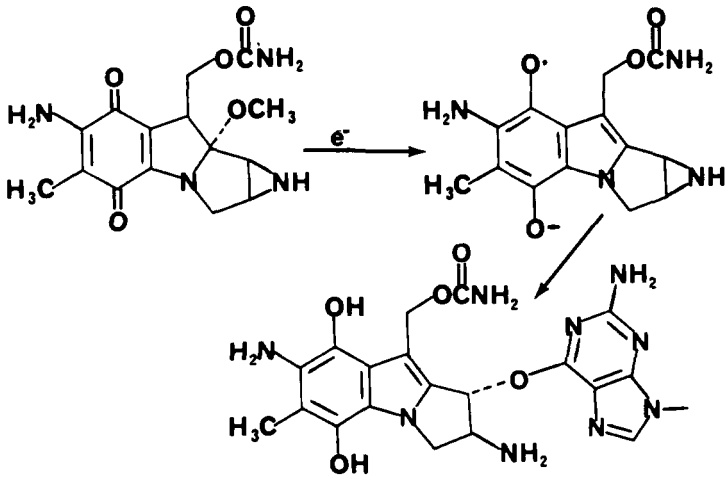

SCHEME 4. Bioactivation of mitomycin C. Monoalkylation of DNA.

produce a gap between the stacked base pairs and the insertion of a flat molecule into this gap. Typical intercalating agents are polycyclic aromatic molecules that can make strong van der Waals interactions with the base pairs. Successful therapeutic agents have this binding augmented by side chains and nuclear substituents that can make ionic or hydrogen bonds with functional groups peripheral to the base pairs. The resulting interactions give the agents prolonged residence time in the DNA (slow exchange rate), which can cause the inhibition of DNA template function in replication or transcription (17). There is controversy over the importance of intercalation to cytotoxicity. Thus, a drug like doxorubicin inhibits DNA polymerase, but it also causes DNA strand cleavage and affects cell membranes. It will take some time to determine the relative importance of factors such as these. However, it still is valuable to consider the effects that intercalation produces in both the DNA and the intercalating agent.

A typical intercalating agent, daunorubicin, is shown in Figure 7. This molecule has three flat rings which can intercalate into double helical DNA. The fourth ring remains outside the helix and its hydroxyl and acetyl groups participate in hydrogen bonding with the bases. No specific binding is apparent for the aminosugar substituent, but it has been suggested that this substituent binds to DNA polymerase and prevents its full operation (18). Figure 8 shows the binding of daunorubicin with a hexanucleotide dimer, as determined by X-ray crystallography (18). It should be noted that the daunorubicin molecule is parallel to the base pairs above and below it, but turned at an angle of almost 90° to them. The hydrogen bonds, one involving a water bridge, also are evident.

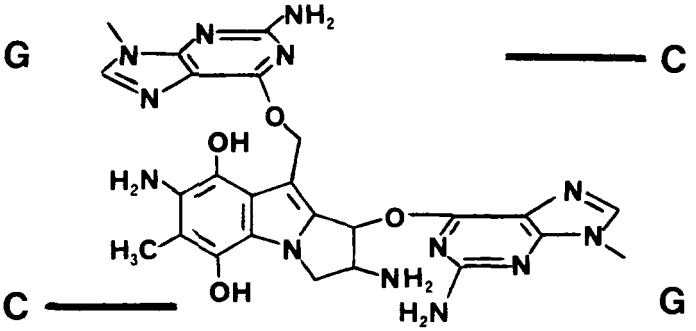

FIGURE 6. Dialkylation of DNA by reduced mitomycin C. Taken from Arora (14). Permission from Pergamon Press.

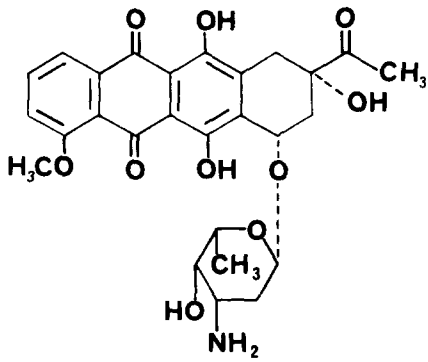

FIGURE 7. Daunorubicin.

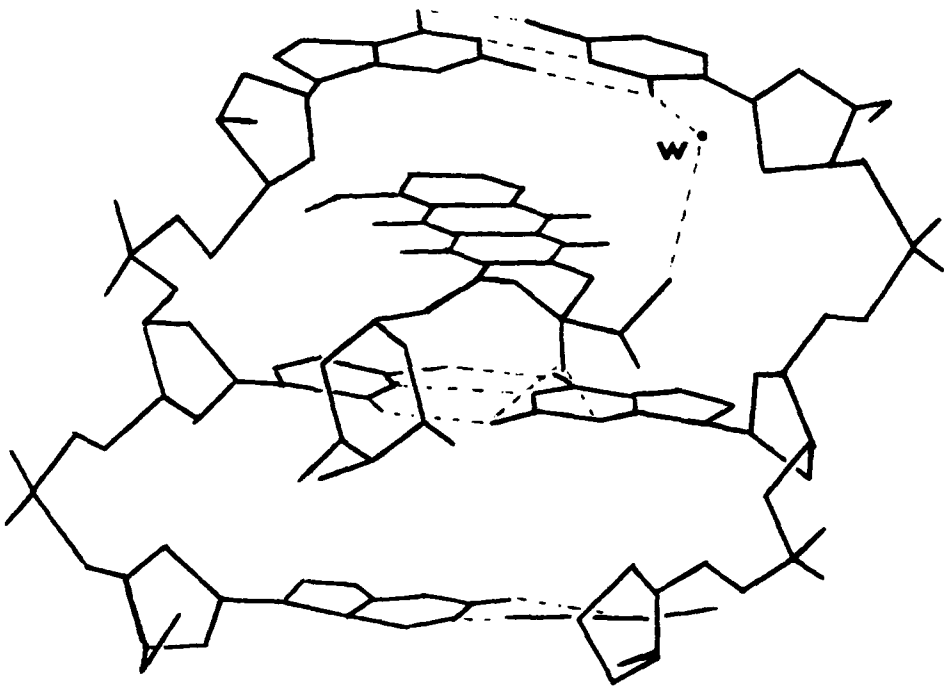

FIGURE 8. Daunorubicin intercalated into a hexanucleotide dimer. The symbol w represents a water molecule and dashed lines indicate hydrogen bonding. Redrawn from Quigley, *et al.* (18). Permission from the authors.

Binding of drugs to DNA by various modes, including intercalation, causes changes in the uv and visible absorption spectra of the drugs. In general, the absorption maximum is shifted to longer wavelength, and it has diminished intensity (17). These effects are apparent in the plot of visible light absorption by actinomycin to which increasing amounts of DNA are added (Figure 9). Such a family of curves usually shows an isosbestic point at which they all intersect. From these families of curves, it is possible to follow the absorbancy changes at a particular wavelength, usually the one at which maximum absorption occurs. Figure 10 shows such a plot for daunorubicin. Using these data and a knowledge of the absorbancy, in the absence of DNA and when all of the drug is bound to DNA (large excess of DNA), it is possible to calculate ratios of the bound and free drug, per DNA base pair, at each concentration used for the absorbancy plot. The resulting ratios can then be used in a Scatchard plot of binding isotherms, which enables one to calculate the apparent binding constant Kapp for the drug-DNA

interaction and the number of binding sites per base pair (15,16). An example of a Scatchard plot for actinomycin binding is shown in Figure 11. In this plot, m is the concentration of free drug and r is the bound drug per base pair. The slope of the linear portion of the curve gives -Kapp and extrapolation to the abscissa gives the number of specific binding sites Bapp. Deviation of the curve from a straight line represents non-specific binding at higher drug concentrations (17).

The physical properties of DNA also are affected by drug binding, including intercalation. Binding increases the stability of the double helix, which means that more

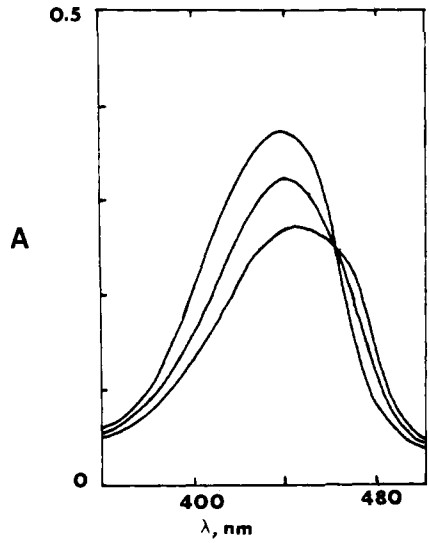

FIGURE 9. Effect on the absorption spectrum of antinomycin due to added calf thymus DNA. Redrawn from Muller and Crothers (17). Permission from *Journal of Molecular Biology*.

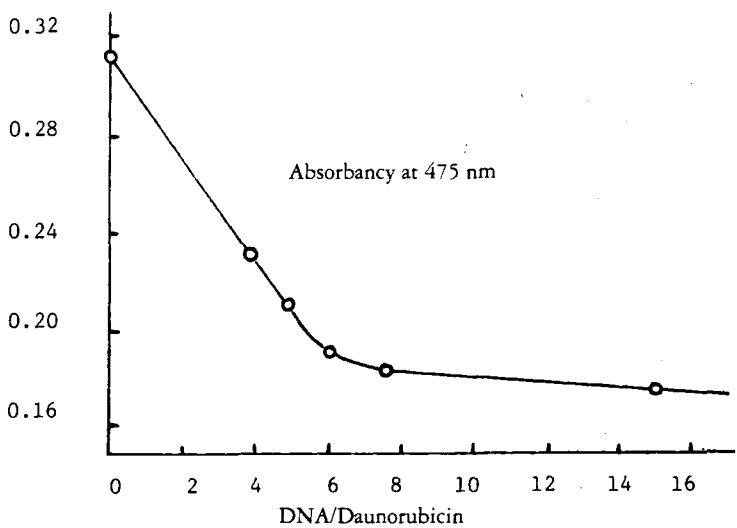

FIGURE 10. Changes in the absorbancy of daunorubicin at 475 nm caused by added DNA. Redrawn from Di Marco (15). Permission from Springer-Verlag.

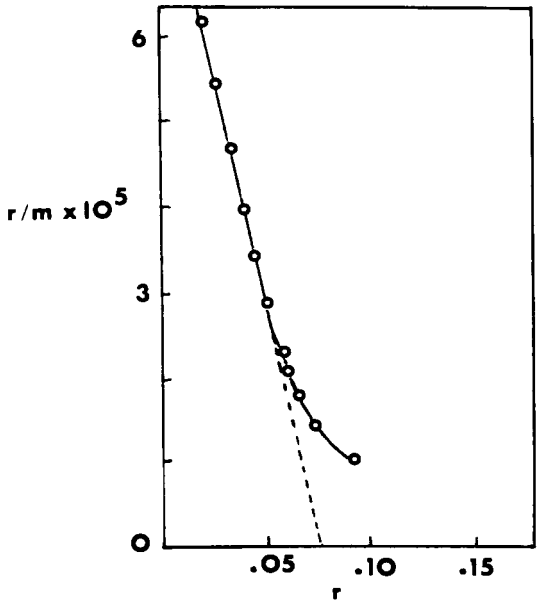

FIGURE 11. Scatchard plot for the binding isotherms of actinomycin with DNA. Redrawn from Muller and Crothers (17). Permission from *Journal of Molecular Biology*.

energy is required for denaturation. Thus, an increase will occur in the thermal denaturation temperature of DNA in solution. This temperature, also known as the melt transition temperature, is obtained conveniently by measuring the ratio of uv light absorption at temperature T (A_To) to that at a standard temperature ($A_{40°}$), chosen as 40° because no denaturation occurs there, and plotting these ratios versus the gradually increasing temperature. As denaturation begins, the light absorption increases because the bases present in single standard DNA absorb more strongly than those still in the double helix. At some particular temperature, a steep increase in the ratio is observed, but the curve levels off when denaturation is complete (Figure 12). The inflection point is chosen as the melt transition temperature (Tm). It is evident how this temperature is increased by the intercalation of daunorubicin. The increase in Tm at a standard drug concentration gives a measure of the relative binding strength of each drug (15,16).

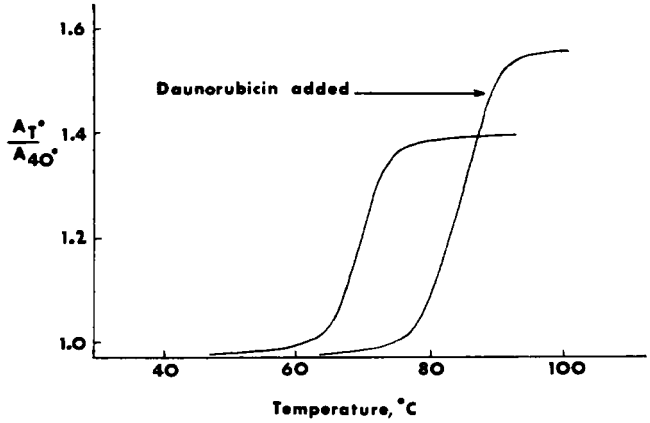

FIGURE 12. Thermal denaturation of DNA in the absence and presence of daunorubicin. Redrawn from Zunino (16). Permission from Elsevier/North Holland.

Another DNA physical property affected by drug binding is the sedimentation rate. Intercalating drugs cause the double helix to become longer and stiffer. These changes are reflected in a slower rate of sedimentation. Drug intercalation into covalently closed circular DNA causes untwisting of the supercoiling. As more drug is added, the sedimentation rate decreases until a minimum is reached at the point of complete untwisting. The addition of still more drug produces supercoiling with the opposite twist, and the sedimentation rate increases (19). Both of these sedimentation effects are shown in Figure 13. In this figure, actinomycin is added to DNA from ØX174 phage. This DNA contains both covalently closed circles and broken circles. The lower curve (triangles) shows the gradual increase in sedimentation rate with added drug for the broken circles whereas the upper curve shows the fall and rise in sedimentation rate experienced by covalently closed circles.

Lengthening and stiffening of DNA also causes an increase in the viscosity of DNA solutions. This effect can be determined conveniently by standard techniques of viscosimetry (17).

In most of the effects described above, it is difficult to establish with certainty that the drug is intercalating rather than binding on the outside of the DNA in one of the grooves (apposition). The unwinding of supercoils in covalently closed circular DNA is the most reliable test of intercalation. Another method that appears to be specific for intercalation is measurement of the chemical shifts in the ^{1}H-nmr spectra of the DNA. In particular the protons involved in N-H---N bonding between base pairs (circled atoms in Figure 14) appear in a region of high deshielding where no other protons interfere. Therefore, the shielding effects caused by the ring currents in polycyclic aromatic intercalating agents can be readily identified and measured. Molecules such as netropsin that bind in the grooves on the outside of the double helix cause small deshielding effects on these protons. The theoretical analysis of the shielding effects caused by intercalating agents is complex, but it has recently been explained with clarity (20). Both the rate of exchange between bound and unbound intercalating agent and the base pair specificity are important to this analysis. Figure 15 shows the theoretical analysis for limiting cases of slow and fast exchange for the examples wherein the base specificity is 2:1 GC at AT

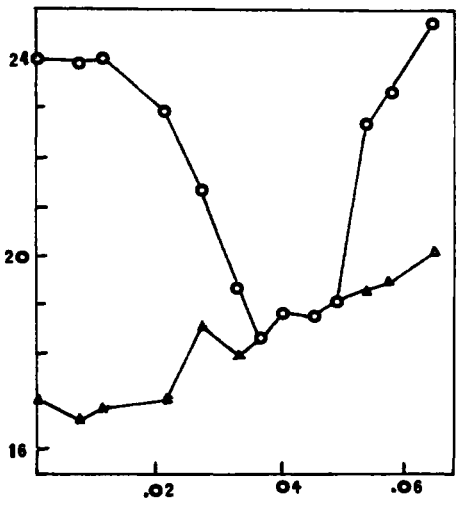

FIGURE 13. Effect of actinomycin on the S_{20} of DNA from X174. Redrawn from Waring (19). Permission from *Journal of Molecular Biology*.

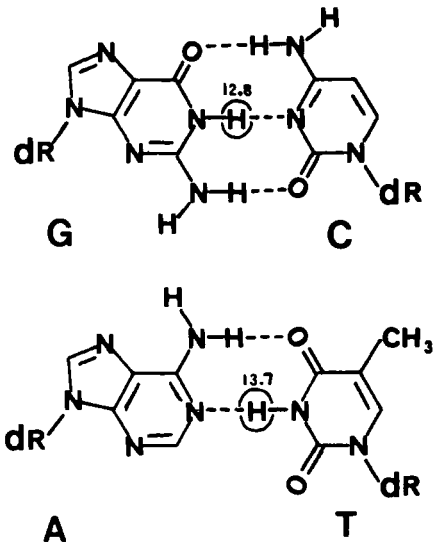

FIGURE 14. Deshielding of Hydrogen-bonded protons between DNA base pairs.

and 2:1 AT to GC. For the slow exchange (slow in comparison to the ^{1}H-nmr process), new peaks appear upfield as the result of shielding by the intercalating agent. The relative heights of the peaks indicate the base specificity. In contrast, intercalating agents in fast exchange show only two peaks which results from averaging of the normal and shielded proton chemical shifts. The base specificity is revealed by the relative distance each peak is shifted from its normal value (20).

Specific examples of effects on the ^{1}H nmr of DNA caused by intercalating agents are illustrated in Figures 16 and 17. In Figure 16, the two-peaks produced by DNA containing intercalated methylharman clearly show a fast exchange rate and GC specificity. As expected from this fast exchange, methylharman is not a particularly effective agent for DNA effects. In contrast, the binding of actinomycin to DNA is seen in Figure 17 to involve GC specificity with slow exchange. This result is consistent with numerous other studies on actinomycin binding. The slow exchange means that actinomycin has a long enough residence time to inhibit DNA functions including replication.

CLEAVAGE OF DNA STRANDS.—A variety of natural products are capable of cleaving DNA strands. This event is cytotoxic; hence, the usefulness of compounds able to cleave DNA will be as antitumor agents. Certain antitumor agents act by a variety of mechanisms in causing cell death. For example, mitomycin C appears to act mainly by alkylation under hypoxic conditions, but in the presence of oxygen and a cytochrome system, it also produces strand scission. Daunorubicin acts by intercalation, strand scission, and by an effect on the cell membrane. Among these mechanisms, the strand scission resulting from free radical generation is thought to be the main cause of cardiotoxicity.

The strand cleavage action of bleomycins has been studied in detail. These remarkable molecules will serve as our main example of the scission process. Figure 18 illustrates the structures of bleomycins A_2 and B_2 (21), which are present in the clinical antitumor product. These structures can be divided into three different regions related to their roles in the mode of action. On the right side of the structures (as illustrated) is a

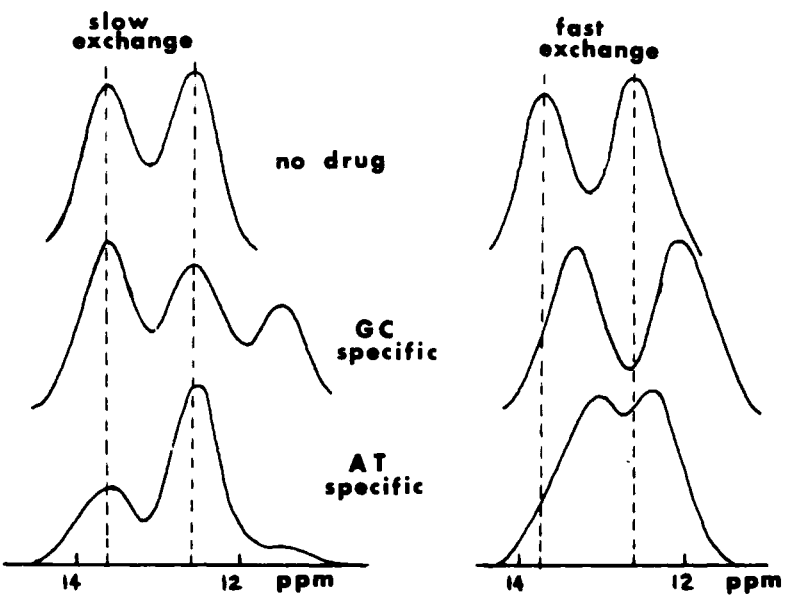

FIGURE 15. Theoretical analysis of the shielding effects of intercalating agents with AT and GC specifity and with fast and slow exchange. Redrawn from Feigon, *et al.* (20). Permission from American Chemical Society.

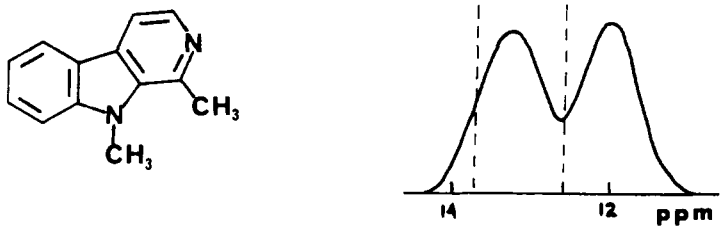

FIGURE 16. Structure and ^{1}H-nmr shielding effect of methylharman. Spectrum redrawn from Reference 20.

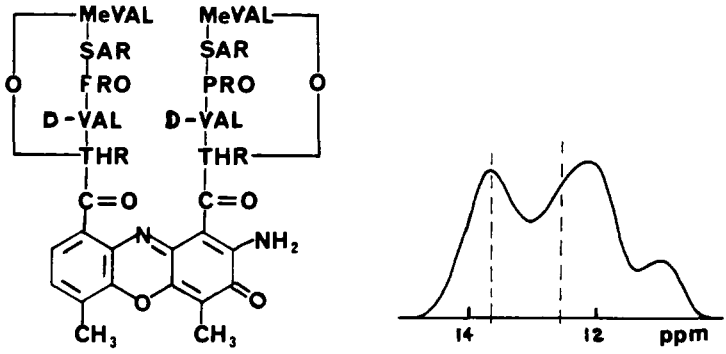

FIGURE 17. Structure and ^{1}H-nmr shielding effect of actinomycin. Spectrum redrawn from Reference 20.

bithiazole unit and a terminal group which bears a positive charge (sulfonium) or will bear a positive charge under physiological conditions (guanidine). The role of these functionalities is to bind to the DNA: the bithiazole unit intercalates and the positively charged center provides binding to the DNA surface. There is a high specificity for guanosine in the DNA (22). The binding unit is connected by the second region, a polypeptide chain, to the third region, which consists of an α-hydroxyhistidine residue bearing two sugars and a highly substituted pyrimidine. This third region is able to form a hexacoordinate complex with metal ions such as Cu(II), Co(II) and Fe(III). As shown in Figure 19, five of the ligands are nitrogen and the sixth is the carbonyl oxygen of a carbamate group on one of the sugars (23). This last ligand binds weakly, and it can be replaced by molecular oxygen. In fact, synthetic bleomycin analogues without the sugars retain most of the DNA cleaving ability of the natural products (24).

Recent studies on the mechanism of bleomycin-induced DNA cleavage have shown that it is based on the hydroxylation of C-4 in a 2-deoxyribose unit. The resulting unit cleaves to a propenal with concomitant strand breakage. Subsequent hydrolysis of this propenal releases guanine. Hydroxylation of the 2-deoxyribose unit takes place by a process analogous to the way in which cytochromes hydroxylate molecules (25). This process is outlined in Scheme 5. Thus, a complex between bleomycin (BLM) and Fe(III) is reduced, possibly by thiols, to give BLM-Fe(II), which binds to DNA. The resulting system takes up oxygen and then undergoes a transition to the oxine $[(FeO)^{+3}]$ containing system. In the latter system, hydroxylation of the DNA by oxygen insertion occurs. Finally, the resulting BLM-Fe(III) complex dissociates from the hydroxylated DNA.

Bleomycins make both single strand cleavage (nicking) and double strand cleavage of DNA. There are several ways in which the results of cleavage can be examined. They involve the use of supercoiled covalently closed circular DNA and the effect that intercalated ethidium has in sensitizing the fluorescence of the bases in DNA. One method is based on the separation of supercoiled and nicked or doubly cleaved DNA on sephadex

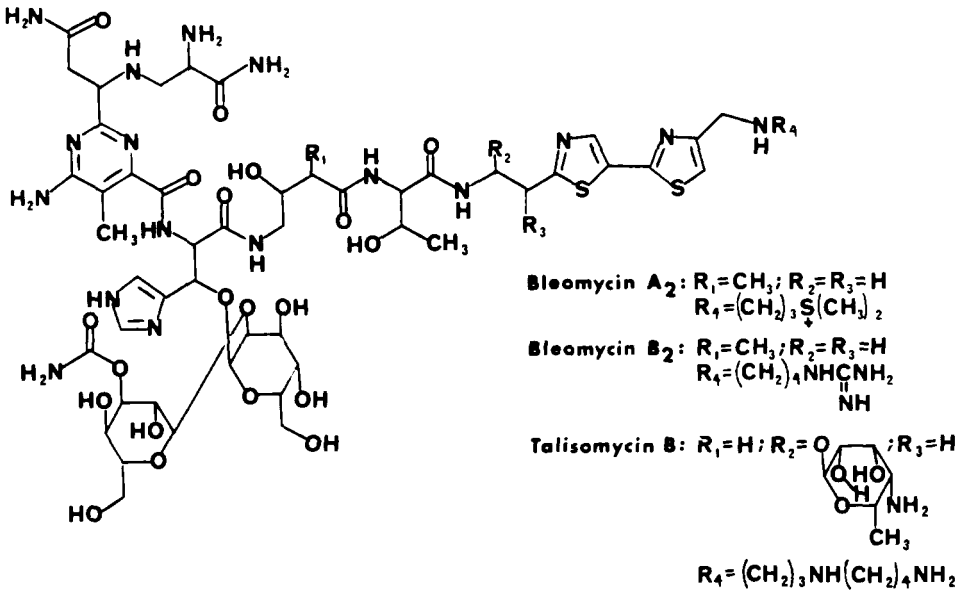

FIGURE 18. Bleomycins and talisomycin.

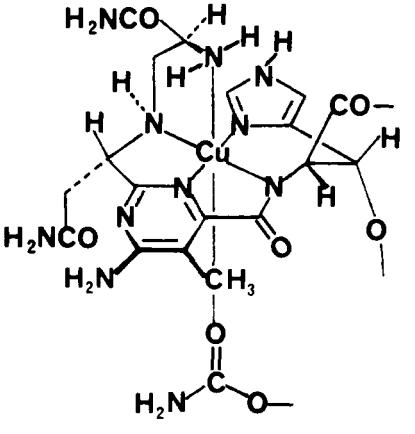

FIGURE 19. Structure of the Cu(II) complex of a bleomycin fragment. Redrawn from Iitaka, *et al.* (23). Permission from Japanese Society for Antibiotics.

chromatography. Another method, illustrated in Figure 20, is based on the detection of single strand cleavage by the difference in fluorescence before and after denaturation (9). When the supercoiled DNA is nicked, it becomes relaxed into a pair of one closed and one open circle, an arrangement which can accommodate increased ethidium intercalation and, consequently, increased fluorescence. However, if this DNA is denatured by heating at pH 12, the duplex does not reform, and the fluorescence falls to zero.

DNA SEQUENCING.—DNA sequencing methods are valuable in determining the locations at which natural products bind to DNA. Essential to these procedures are the isolation of unique DNA fragments from genomes by the use of type II restriction endonucleases. These enzymes are isolated from a variety of bacteria, and they are com-

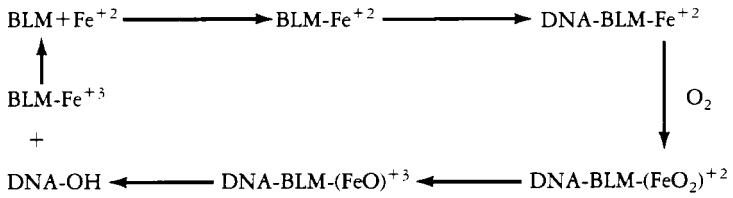

SCHEME 5. Hydroxylation of DNA by bleomycin, iron, and molecular oxygen.

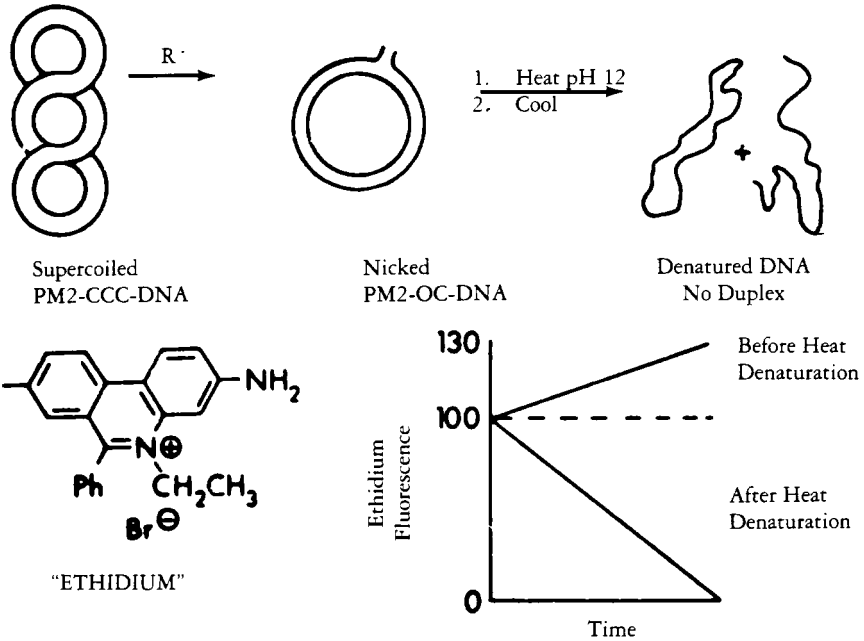

FIGURE 20. Detection of single strand cleavage of DNA by the ethidium fluorescence method. Reproduced from Lown (9). Permission from Academic Press.

mercially available. Restriction enzymes recognize self complimentary (pallindromic) sequences in DNA. As an example, HinfI recognizes the sequence $^{(5')}_{(3')}$GANTC / CTNAG and cuts both strands to yield identical ends $^{(5')}_{(3')}$ANTC / G. Such fragments are treated with enzymes capable of introducing specific radioactive phosphate labels from appropriate precursors such as [γ-^{32}P]ATP. Polynucleotide kinase labels the 5′ end, and DNA polymerase I labels the 3′ end. A secondary restriction enzyme digest within the double end-labeled fragment then generates a unique single end-labeled fragment, which can be isolated by gel electrophoresis and autoradiography.

Maxam and Gilbert (26) have used the above methods, in combination with specific

TABLE 1. Base-Specific Cleavage Reactions for DNA Sequencing[a]

Cleavage	Reagent for Base Modification	Reagent for Strand Cleavage
G	dimethyl sulfate	piperidine
G+A	acid	piperidine
C+T	hydrazine	piperidine
C	hydrazine+salt	piperidine

[a]Abstracted from Maxam and Gilbert (26).

chemical treatments designed to cleave DNA in a base-dependent manner, to sequence DNA molecules. One such treatment, methylation followed by base, is specific for guanine. It was discussed in detail above. Other specific cleavage reactions are listed in Table 1. They include cleavage of G+A sites, C+T sites, and C sites. After these cleav-

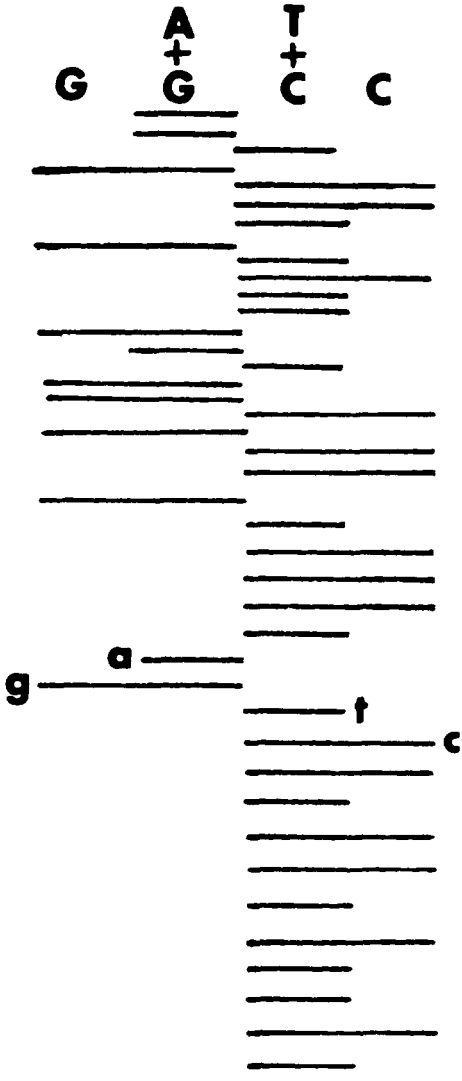

FIGURE 21. Schematic representation of a gel from the Maxam-Gilbert method for DNA sequencing.

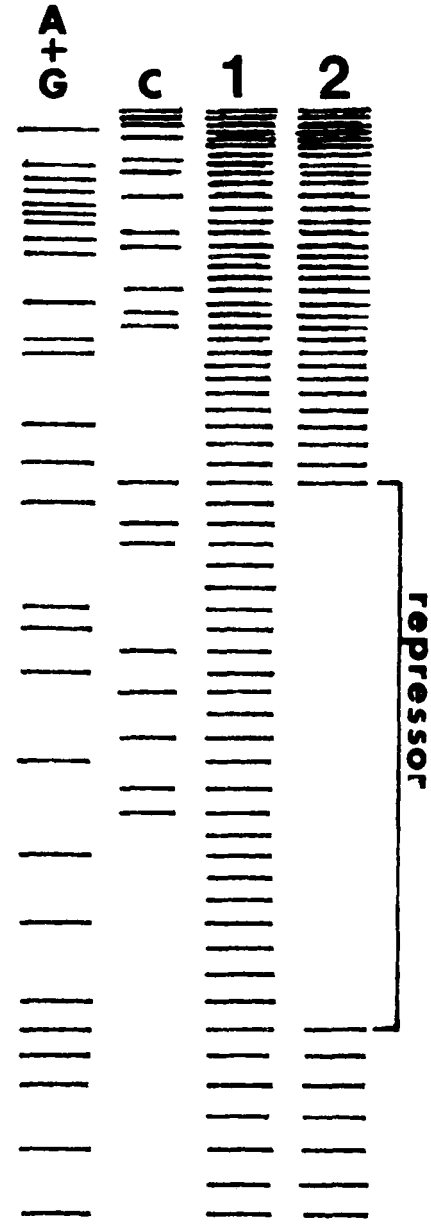

FIGURE 22. Schematic representation of a gel from DNA sequencing by the Galas and Schmitz "footprinting" method. This shows the degradation of the lactose operton region of DNA in the absence and presence of the repressor of the operon. Based on Reference 27.

ages, electrophoresis through polyacrylamide gels sorts the nested sets of small polynucleotides according to size. The smaller a fragment is, the faster it migrates in the gel. Figure 21 shows in schematic form a gel obtained from Maxam-Gilbert sequencing. The order of bases can be discerned clearly from their migration distances and the cleavage conditions that produced them.

Molecules that bind strongly to DNA can protect their binding sites from cleavage by the sequencing reagents. The resulting gel electrophopresis pattern will have one or more gaps corresponding to the binding sites, which will indicate where binding occurs in the DNA sequence. This "footprinting" method has been developed by Galas and Schmitz, and by others (27). Figure 22 shows in schematic form the results of protection of a segment of the lactose operon by its repressor.

Depending on the nature of the drug binding to DNA, specific variations in the sequencing methods have been devised to "footprint" the binding site. For a drug that causes strand scission, it only is necessary to separate the strands, label them, and analyze the residues on a high resolution gel. An example of the technique is shown in Figure 23, wherein the sequence specificity for strand scission by bleomycin A_2 is compared with that of a different but structurally related compound, talisomycin A (Figure 18). The amount of cleavage is indicated by densitometric readings of the gels. It can be seen in the sequence code given in the legend for Figure 23 that major cleavages occur next to guanines. Although bleomycin A_2 and talisomycin cleave at the same site, there is clearly a difference in the relative amounts of cleavage at these sites. The presence of an additional sugar unit in the structure of talisomycin A probably is responsible for this difference (28).

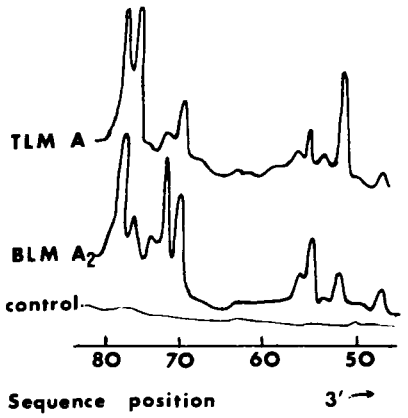

FIGURE 23. Densitometric readings of gels from the cleavage of DNA by a bleomycin and a talisomycin. Redrawn from Mirabelli, *et al.* (28). Permission from the American Society for Cancer Research. The DNA sequence is as follows:

```
5' ACTGTGAATGCGCAAACCAACCCTTGGCAGAACAT 3'
   TGACACTTACGCGTTTGGTTGGGAACCGTCTTGTA
   |           |           |           |
   80          70          60          50
```

The binding sites of covalently bound drugs can be determined by degrading the DNA with an exonuclease. This enzyme will not cleave at the place where covalent binding occurs. After strand separation, the drug must be removed from the DNA before sequencing can be carried out. Equilibrium binding drugs cannot withstand the

action of exonucleasis; consequently, another method for "footprinting" is required. This method is based on the stability of their binding to endonucleases, which will cleave the DNA at places other than where the drug is bound. Figure 24 shows the

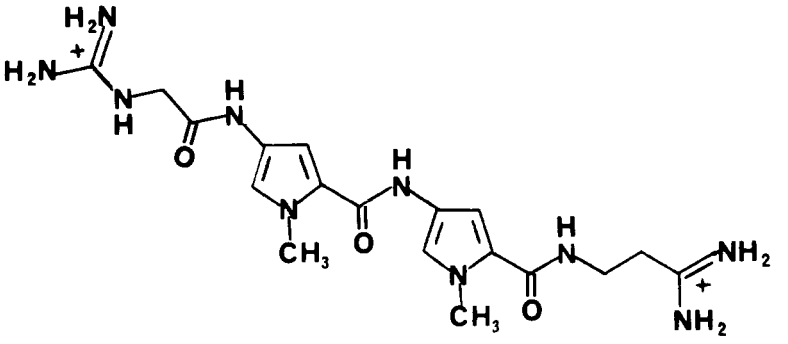

FIGURE 24. Netropsin.

structure of netropsin, a compound that binds in the minor groove with high specificity for AT base pairs. The cleavage pattern of DNA complexed with netropsin is given in Figure 25. It clearly shows protection of the AT rich region from positions 60 through 74. Also shown in this figure is the protection afforded by actinomycin, an intercalating agent with GC specificity (29).

When a DNA sequence is known, the regions protected by a drug can be determined conveniently by the use of newly introduced cleavage methods such as Dervan's reagent, (methidiumpropyl-EDT) iron (II) (Figure 26). This reagent is based on the structure of bleomycin in that it has an intercalating group (methidium) joined by a

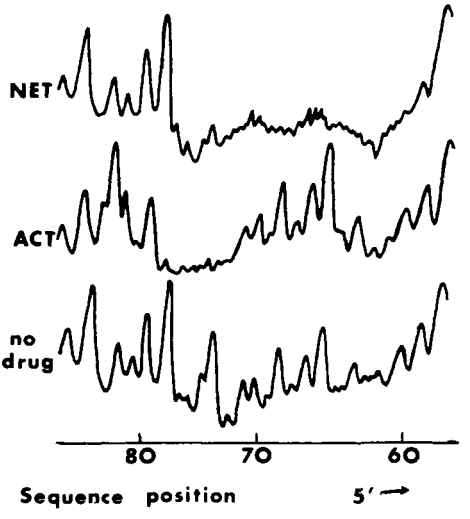

FIGURE 25. Densitometric readings of gels from the cleavage of DNA bound to netropsin or actinomycin or with no drug added. Redrawn from Lane, *et al.* (29). Permission from the authors. The DNA sequence is as follows:

```
3' TACTGCTACTCGCGTAACAATCTAAAGTATG 3'
   ATGACGATGAGCGCATTGTTAGATTTCATAC
        |          |          |
       80         70         60
```

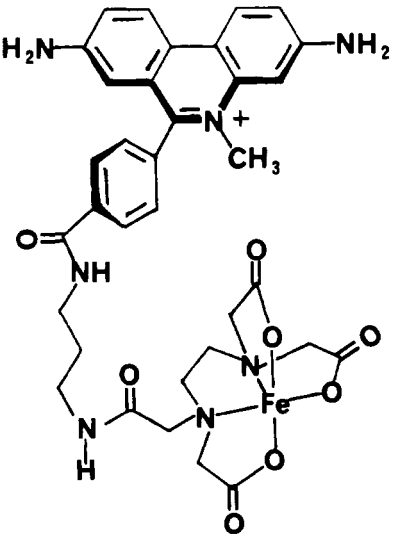

FIGURE 26. (Methidiumpropyl-EDT) iron (II).

short tether to EDTA chelated with iron (30). The resulting system generates strand-cleaving radicals in close proximity to the DNA. No selectivity is possible with this particular reagent; it cleaves at every unprotected site. Figure 27 shows the result of

FIGURE 27. Regions of DNA protected by distamycin from cleavage with (methidiumpropyl-EDT) iron (II). Based on Reference 31.

cleaving DNA protected by distamycin A, another drug that binds in the minor groove with AT specificity. It should be noticed that the "footprints" caused by distamycin A are asymmetric with respect to the two DNA strands. This occurs because the winding of distamycin A in the minor groove results in assymetric protection from the cleaving reagent (31).

Although (methidiumpropyl-EDT) iron (II) shows no specificity in cleaving DNA, it has been possible to develop related reagents that do have specificity. This is done by replacing the methidium unit with a larger unit known to bind in a specific manner. Thus, the iron (II) complex of distamycin-EDTA (Figure 28) binds selectively to the

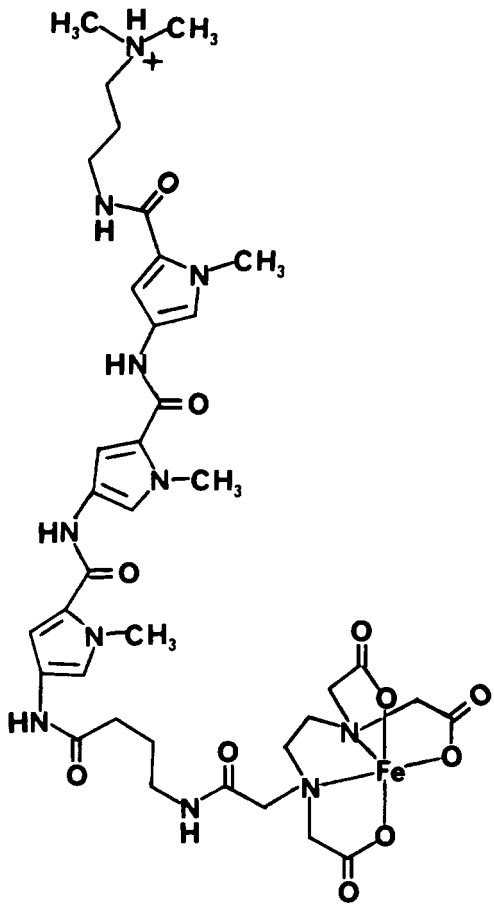

FIGURE 28. (Distamycin-EDTA) iron (II).

AT-rich region of DNA and cleaves next to this region (32). Figure 29 shows schematically the predominant cleavage sites produced by this reagent in a double-helical DNA strand. It is anticipated that the application of this kind of effect to reagents with larger binding areas will produce even more selective cleavage. One example already known is the analogue with two distamycin units in tandem (32).

FIGURE 29. Predominant cleavage sites in DNA produced by (distamycin-EDTA) iron (II). Redrawn from Schultz and Dervan (32). Permission from American Chemical Society.

A very recent example of a natural product with alkylating ability and binding specificity extending over five base pairs was found in the antitumor antibiotic CC-1065 (33). This molecule (Figure 30) lies in the minor grove of double helical DNA and has two classes of binding sites: 5′ AAAAA and 5′ PuNTTA, where Pu is either purine and N is any nucleotide base. The cycloproppane ring of CC-1065 is opened by nucleophilic attack of N^3 of adenine and this results in the alkylation.

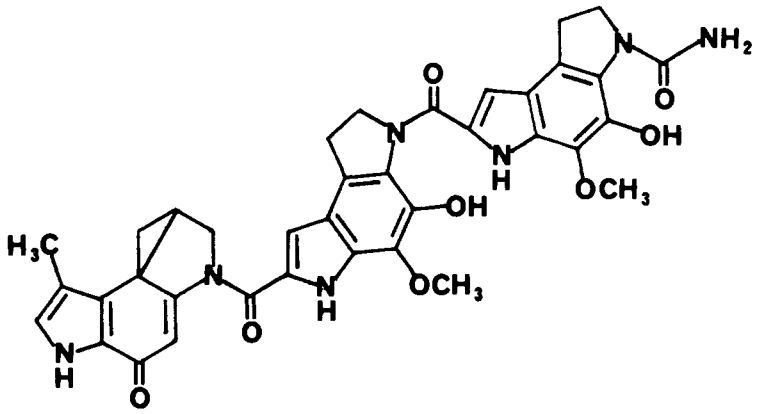

FIGURE 30. Antibiotic CC-1065.

In summary, it is apparent that substantial progress has been made in understanding the chemical and physical effects of drug binding to DNA. It also is possible to determine conveniently the location and binding specificity of these small molecules. This information can then be used in the rational construction of selective cleaving agents. Such tools should become increasingly important in nucleic acid research.

ACKNOWLEDGMENTS

The author expresses sincere thanks to Professors Laurence H. Hurley and Stephen R. Byrn who read the manuscript and made helpful suggestions.

LITERATURE CITED

1. R.E. Franklin and R.G. Gosling, *Acta Crystallogr.*, **6**, 673 (1953).
2. A.H. J. Wang, S. Fugie, J.H. van Boom, and A. Rich, *Proc. Natl. Acad. Sci. USA*, **79**, 3968 (1982).
3. S. Arnott and D.W.L. Hukins, *Nature*, **224**, 886 (1969).
4. A.H.J. Wang, G.J. Quigley, F.J. Kalpak, J.L. Crawford, J.H. van Boom, G. van der Marel, and A. Rich, *Nature*, **282**, 680 (1979).
5. H. Weintraub, A. Worcel, and B. Alberts, *Cell*, **9**, 409 (1976).
6. H.M. Sobell, "DNA Dynamics and Drug Intercalation," in: *Molecular Actions and Targets for Cancer*

Chemotherapeutic Agents. Ed. by A.C. Sartorelli, J.S. Lazo, and J.R. Bertino, New York: Academic, 1981, pp. 132-133.
7. A. Nordheim, W.M. Hao, G.N. Wogan, and A. Rich, *Science*, **219**, 1434 (1983).
8. C.J. Chang, J.D. Gomes, and S.R. Byrn, *J. Org. Chem.*, **48**, 5151 (1983).
9. J.W. Lown, "The Molecular Mechanism of Antitumor Action of the Mitomycins," in: *Mitomycin C, Current Status and New Development*. Ed. by S.K. Carter and S.T. Crooke, New York: Academic, 1979, p. 17.
10. V.N. Iyer and W. Szybalski, *Science*, **145**, 55 (1964).
11. K.A. Kennedy, S.G. Sligar, L. Polamski, and A.C. Sartorelli, *Biochem. Pharmacol.*, **31**, 2011 (1982).
12. Y. Hashimoto, K. Shudo, and T. Okamoto, *Tetrahedron Lett.*, **23**, 677 (1982).
13. M. Tomasz, R. Lipman, J.K. Snyder, and K. Nakanishi, *J. Am. Chem. Soc.*, **105**, 2059 (1983).
14. S.K. Arora, *Life Sci.*, **24**, 1519 (1979).
15. A. Di Marco, "Daunomycin and Related Antibiotics," in: *Antibiotics, Vol. 1*. Ed. by D. Gottlieb and P.D. Shaw, Berlin: Springer-Verlag, 1967, pp. 190-210.
16. F. Zunino, R. Gambetta, A. DiMarco, and A. Zaccara, *Biochim. Biophys. Acta*, **277**, 489 (1972).
17. W. Muller and D.M. Crothers, *J. Mol. Biol.*, **35**, 251 (1968).
18. G.J. Quigley, A.H.J. Wang, G. Ughetto, G. van der Marel, J.H. van Boom, and A. Rich, *Proc. Natl. Acad. Sci. USA*, **77**, 7204 (1980).
19. M. Waring, *J. Mol. Biol.*, **54**, 247 (1970).
20. J. Feigon, W.A. Denny, W. Lenpin, and D.R. Kearns, *J. Med. Chem.*, **27**, 450 (1984).
21. T. Takita, Y. Muraoka, T. Nakatani, A. Fujii, Y. Umezawa, H. Naganawa, and H. Umezawa, *J. Antibiot.* (Tokyo), **31**, 801 (1978).
22. H. Kasai, H. Naganawa, T. Takita, and H. Umezawa, *J. Antibiot.* (Tokyo), **31**, 1316 (1978).
23. Y. Iitaka, H. Nakamura, T. Nakatani, Y. Muraoka, A. Fujii, T. Takita, and H. Umezawa, *J. Antibiot.* (Tokyo), **31**, 1070 (1978).
24. Y. Aoyagi, H. Suguna, N. Murugesan, G.M. Ehrenfeld, L.-H. Chang, T. Ohgi, M.S. Shekhani, M.P. Kirkup, and S.M. Hecht, *J. Am. Chem. Soc.*, **104**, 5237 (1982).
25. R.M. Burger, S.B. Horwitz, and J. Peisach, 188th National Meeting of the American Chemical Society, Phila., PA., August, 1984. Abstracts BIOL 114.
26. A.M. Maxam and W. Gilbert, *Methods Enzymol.*, **65**, 499 (1980).
27. D.J. Galas and A. Schmitz, *Nucleic Acids Res.*, **5**, 3157 (1978).
28. C.K. Mirabelli, W.G. Beattie, C.H. Huang, A.W. Prestayko, and S.T. Crooke, *Cancer Res.*, **42**, 1399 (1982).
29. M.J. Lane, J.C. Dabrowiak, and J.N. Vournakis, *Proc. Natl. Acad. Sci. USA*, **80**, 3260 (1983).
30. R.P. Hertzberg and P.B. Dervan, *J. Am. Chem. Soc.*, **104**, 313 (1982).
31. M.W. Van Dyke and P.B. Dervan, *Cold Spring Harbor Symp Quant. Biol.*, **47**, 347 (1982).
32. P.G. Schultz and P.B. Dervan, *J. Am. Chem. Soc.*, **105**, 7748 (1983).
33. L.H. Hurley, V.L. Reynolds, D.H. Swenson, G.L. Petzold, and T.A. Scahill, *Science*, **226**, 843 (1984).